

# **HEART-Watch: A multimodal physiological dataset from a Google Pixel Watch across different physical states**

Jathushan Kaetheeswaran

Institute of Biomedical Engineering, University of Toronto, Canada and KITE Research Institute, University Health Network, Canada

Boyi Ma

Institute of Biomedical Engineering, University of Toronto, Canada and KITE Research Institute, University Health Network, Canada

Ali Abedi

Institute of Biomedical Engineering, University of Toronto, Canada and KITE Research Institute, University Health Network, Canada

Milad Lankarany

Institute of Biomedical Engineering, University of Toronto, Canada and KITE Research Institute, University Health Network, Canada

Shehroz S. Khan

College of Engineering and Technology, American University of the Middle East, Egaila, 54200, Kuwait

Consumer-grade smartwatches offer a new personalized health monitoring option for general consumers globally as cardiovascular diseases continue to prevail as the leading cause of global mortality. The development and validation of reliable cardiovascular monitoring algorithms for these consumer-grade devices requires realistic biosignal data from diverse sets of participants. However, the availability of public consumer-grade smartwatch datasets with synchronized cardiovascular biosignals is limited, and existing datasets do not offer rich demographic diversity in their participant cohorts, leading to potentially biased algorithm development. This paper presents HEART-Watch, a multimodal physiological dataset collected from temporally synchronized wrist-worn Google Pixel Watch 2 electrocardiogram (ECG), photoplethysmography, and accelerometer signals from a diverse cohort of 40 healthy adults across three physical states - sitting, standing and walking with reference chest ECG. Intermittent upper arm blood pressure measurements and concurrent biosignals were

collected as an additional biomarker for future research. The motivation, methodology, and initial analyses of results are presented. HEART-Watch is intended to support the development and benchmarking of robust algorithms for cardiovascular analyses on consumer-grade smartwatches across diverse populations.

## 1 INTRODUCTION

Remote cardiovascular monitoring has advanced significantly in the past decade, with the release of novel consumer-grade smartwatches and artificial intelligence (AI) algorithms. Given that cardiovascular diseases (CVDs) continue to be the primary cause of mortality globally [1,2], continuous monitoring with commercial smartwatches can be leveraged to identify risk factors, promote healthier lifestyles, and reduce burdens on healthcare systems by encouraging self-monitoring habits [3–5]. Modern smartwatches integrate electrocardiogram (ECG), photoplethysmography (PPG), and accelerometer (ACC) sensors to noninvasively acquire physiological signals for cardiovascular analysis [6,7]. The rapid increase in demand for accessible health monitoring tools has propelled the smartwatch industry to an estimated global market value of \$39 billion USD by 2034 [8], showcasing the widespread integration of these tools into the lives of the general public. Clinicians are beginning to incorporate data from these wearables into clinical consultations, such as for atrial fibrillation (AF) screenings [9,10].

Despite their increasing prevalence in consumer’s medical practices and personal health awareness [11–13], consumer-grade smartwatches are not always classified as medical-grade devices, exempting them from rigorous and transparent validation studies [6,7,14–16]. For instance, heart rate (HR) estimation on Google’s WearOS uses PPG and ACC sensors which are exempt from FDA oversight for market release [6,7]. This regulatory context raises concerns about the validity and reliability of cardiovascular metrics derived from these sensors. Smartwatches that contain medical-grade sensors or functionality, such as those with ECG, can also receive expedited FDA clearance by demonstrating substantial equivalence to existing predicate devices rather than undergoing strict premarket approval applications [6,17]. Recently, the Apple Watch obtained FDA clearance for an AI-based hypertension-notification feature by demonstrating substantial equivalence to Viz HCM – an algorithm operating on 12-lead ECGs – despite the Apple feature operating on wrist-based PPG [18,19]. This example illustrates that regulatory clearance does not necessarily require substantial equivalence using consumer-grade smartwatch sensors and data; rather, it may be granted by demonstrating similar intended use and performance.

Robust validation of consumer-grade smartwatches is critical given the limitations of the embedded sensors on wearable devices. The ECG, PPG, and ACC signals collected by wrist-worn devices are vulnerable to quality issues, particularly

during physical activity, such as motion artifacts, signal noise and sensor displacements, reducing their effectiveness for individuals across regular daily activities [6,20–22]. Modern smartwatches are often deployed with AI algorithms that are trained and/or validated on smartwatch datasets [23–25], indicating that the quality of these datasets dictate real-world performance. A persistent barrier for translation of consumer-grade smartwatch algorithm performance from clinical studies to real-world settings is the limited demographic diversity in training and validation cohorts [6,26]. A recent scoping review on wearables for real-time cardiovascular monitoring found that studies performing validation tests only provided general demographic information rather than detailed characteristics such as height, weight, or race, limiting fairness assessments of developed algorithms [27,28]. Validation performed on young, healthy, racially homogenous adults will not capture the variability in cardiovascular biomarkers for other populations, highlighting the need for diverse datasets with a variety of skin tones, body types, and socioeconomic backgrounds [6,14,15,17]. Training and evaluating smartwatch algorithms in realistic, noise-contaminated data from a diverse demographic cohort is crucial for ensuring that these algorithms still perform well through regular activities for the general population [29]. Additionally, many existing consumer-grade smartwatch datasets provide aggregate measures such as HR rather than raw sensor values due to restrictions placed on data access [30]. When raw sensor data is provided, existing datasets are often limited to PPG and/or ACC signals, but not smartwatch ECGs longer than 30 seconds, limiting frequency-based analysis. Based on these factors, a critical gap remains: open, multimodal datasets from consumer-grade smartwatches with rich participant demographics and recordings across physical states are scarce.

To address this gap, this work presents HEART-Watch, a dataset of time-aligned ECG, PPG, and ACC signals from a consumer-grade smartwatch alongside reference chest ECG across a diverse cohort of healthy adults. Data was collected across sitting, standing, and walking physical states to enable the development of new smartwatch algorithms for measuring cardiovascular biomarkers, such as HR and heart rate variability (HRV), that are robust to common issues such as motion artifacts and signal saturation [31]. Furthermore, cuff blood pressure (BP) readings and simultaneous smartwatch ECG, PPG, and ACC recordings were conducted between physical states as an additional benchmark for research. The remainder of this paper details the rationale for this work, data acquisition methodology and validation of biosignals, with visualizations and potential use cases highlighted.

## 2 RELATED WORK

A summary of publicly available non-synthetic physiological datasets from consumer-grade smartwatches is provided in Table 1. Datasets were excluded if (i) raw signals or aggregate measures were not provided, (ii) the focus of the work was not cardiovascular analysis for awake, healthy adults, (iii) the data collection involved invasive, custom or prototype devices, or (iv) authors did not provide data availability statements or clearly stated that data was not available to researchers (e.g., the Apple Heart Study [24] and Fitbit Heart Study [23]).

The main limitation of existing datasets is the collection and duration of smartwatch ECG recordings, with only two datasets, SmartHeartWatch and SMART Start, providing this modality [32]. Due to the restrictions on data exports with consumer-grade smartwatches, existing datasets containing smartwatch ECGs are restricted to short recordings, typically 30 seconds, as these are often the default settings in traditional applications [33]. The lack of publicly available prolonged smartwatch ECGs is also likely due to the technical challenges concerning wrist-based ECG recordings, which requires users to maintain constant contact with the opposite hand’s index finger for accurate signal acquisition [34,35]. Despite these limitations, smartwatch ECGs provide more clinical value for physicians who more willing to diagnose based on these tracings compared to PPG tracings, highlighting the need for this modality [10].

Additionally, consumer-grade devices generally make it challenging to access raw sensor data, so existing datasets often provide aggregate measures. While these aggregate measures can be used for analyses and are provided in several existing datasets, the algorithms that generate these results are usually proprietary and undisclosed, limiting reproducibility and transparency [30]. Moreover, demographic information is consistently underreported in these datasets, with only two reporting any details regarding racial diversity [21,36–38] and only three providing height and weight information [39–43]. Robust algorithms for general consumers require datasets that reflect the heterogeneity that exists in the real-world, however, many existing datasets do not place a large emphasis on this aspect during data collection. Finally, older adults are rarely included in existing smartwatch datasets such as GalaxyPPG, which offers long-term, semi-naturalistic recordings but only for young adults below the age of 30 [59]. The inclusion of older adults for smartwatch datasets is relevant as this population is more susceptible to cardiovascular health risks and would benefit more from monitoring algorithms that can account for aging factors such as lower skin perfusion and increased arterial stiffness [7,44,45].

HEART-Watch is unique from existing cardiovascular datasets by providing raw sensor values rather than any aggregate measures, as well as prolonged smartwatch ECG recordings. To the best of our knowledge, HEART-Watch is

the first research dataset to provide consumer-grade smartwatch ECGs of 4 minutes across sitting, standing, and walking physical states. The inclusion of three physical states allows this work to align well with existing datasets that focus on semi-naturalistic signal acquisition to evaluate real-world performance of consumer-grade smartwatches. The availability of reference cuff BP measurements and accompanying biosignals also enables new research using a consumer-grade smartwatch, such as for pulse waveform analysis incorporating prolonged smartwatch ECGs. Finally, HEART-Watch is distinct from existing works by providing semi-naturalistic smartwatch data for a diverse adult cohort ( $n = 40$ ), including older adults up to 75 years old, with race, height, and weight reported for each participant.

Table 1: Literature review of available consumer-grade smartwatch datasets for non-synthetic physiological data from awake, healthy adults. Modalities should be considered smartwatch-derived unless indicated. A ‘—’ indicates that the information was not readily reported.

Reference	Number of participants (F/M)	Mean age (standard deviation) years	Racial categories reported (n)	Height and/or weight reported?	Smartwatch models	Data modalities	Duration	Physical states	Data availability
Bent et al. 2020 [21,36]	53 (32/21)	25.6 (—)	4	—	Apple Watch				
					4, Fitbit				
					Charge 2,			Sitting,	
					Garmin			Paced deep	
					Vivosmart 3,	Chest		breathing,	Data use
					Xiaomi	HR,	1-5 minutes	Walking,	agreement
					Miband 3,	HR		Typing	
					Empatica E4,				
					Biovotion				
					Everion				
Reece et al. 2021 [43]	23 (10/13)	23.6 (3.2)	—	✓	Apple Watch 4, Garmin	Chest HR, HR	57 minutes	Sitting, Everyday activities,	Upon request

Reference	Number of participants (F/M)	Mean age (standard deviation) years	Racial categories reported (n)	Height and/or weight reported?	Smartwatch models	Data modalities	Duration	Physical states	Data availability
					Forerunner 735XT			Walking, Jogging, Running, Cycling	
Sarhaddi et al. 2022 [46]	28 (14/14)	32.5 (6.6)	—	—	Samsung Gear Sport	Chest ECG, PPG	24 hours	Free-living	Data use agreement
SmartHeartWatch 2022 [32]	18 (11/7)	56.0 (20.0)	—	—	Apple Watch 7, Withings ScanWatch	ECG	30-50 seconds	Resting, Recovery	Unclear
SMART Start 2023 [32]	28 (28/0)	34.0 (4.0) years	—	—	Withings ScanWatch	ECG	30-50 seconds	Resting	Unclear
Biswas and Ashili 2023 [37]	1 (0/1)	48.0 (—)	1	—	Fitbit version 2	HR	1 month	Free-living	Subscription
Jaiswal et al. 2024 [47]	32 (—)	—	—	—	Samsung Galaxy Watch 4	Chest ECG, PPG	3 minutes	Sitting, Standing, Walking	Upon request
Baigutanova et al. 2025 [39,40]	49 (25/24)	28.4 (5.9)	—	✓	Samsung Galaxy Active 2	ACC, HR, PPG	4 weeks	Free-living	Open access
GalaxyPPG 2025 [38,48]	24 (12/12)	23.3 (2.0)	1	—	Samsung Galaxy Watch 5	Chest ECG, ACC,	> 1 hour	Social stress activities,	Open access

Reference	Number of participants (F/M)	Mean age (standard deviation) years	Racial categories reported (n)	Height and/or weight reported?	Smartwatch models	Data modalities	Duration	Physical states	Data availability
						HR, PPG		Everyday activities	
Ravanelli et al. 2025 [41,42]	26 (14/12)	30.1 (14.2)	—	✓	Fitbit Charge 5, Bangle.js2	Chest HR, HR	24 hours	Free-living	Open access
HEART-Watch (this paper)	40 (23/17)	44.2 (21.0)	8	✓	Google Pixel Watch 2 (2022)	Chest ECG, ACC, PPG, Cuff BP	4 minutes	Sitting, Standing, Walking	Data use agreement

### 3 METHODS

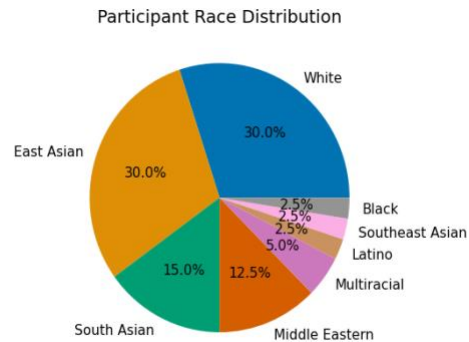
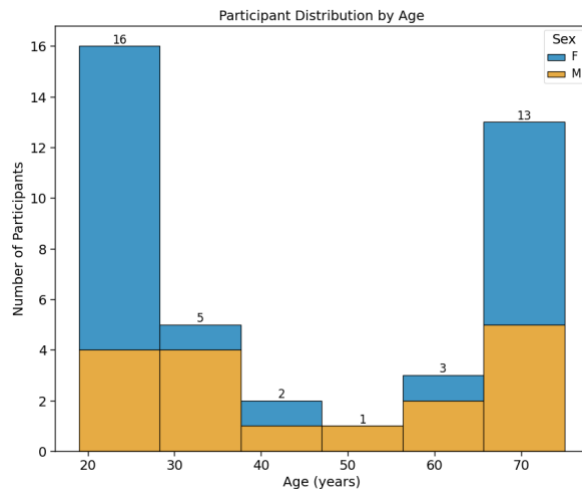
#### 3.1 Ethics Approval

This study was reviewed and approved by the University Health Network (UHN) Research Ethics Board (UHN REB #24-5559) on August 2<sup>nd</sup>, 2024. Recruitment was conducted through the KITE Research Institute, UHN's Study Recruitment webpage open to the public [49], on social media, and via physical posters at several UHN-affiliated hospitals. Participants provided written informed consent to the release of their de-identified data through a control-accessed database prior to data collection.

#### 3.2 Participants

Forty healthy adults (23 females, 17 males, age range = 19 – 75 years, age mean  $\pm$  age standard deviation = 44.2  $\pm$  21.0 years) were recruited to participate in this study from May – July 2025. Participants were included if they were 18 years

or older, able to perform light physical activities without assistance, had intact skin at sensor placement sites, and no self-reported history of disease that could affect breathing or HR. The inclusion and exclusion criteria were developed to recruit a diverse set of healthy participants that did not have morbidities that may affect cardiovascular biomarkers. Demographic information such as age, sex, height, weight, and race was collected at the start of each session. Figure 1 highlights the inclusion of older adults, with 40% ( $n = 16$ ) of participants being 55 years or older. In addition to older adults, HEART-Watch contains a large cohort of younger adults, with 52.5% ( $n = 21$ ) below 40 years old. These distributions support age-based comparisons of smartwatch algorithms. Participants self-identified across eight racial groups, with the largest groups being East Asian ( $n = 12$ ), White ( $n = 12$ ), South Asian ( $n = 6$ ) and Middle Eastern ( $n = 5$ ). This racial diversity is important for cardiovascular algorithm generalizability, and allows for fairness comparisons between groups during validation [28]. Body-type diversity is also reflected in the height-weight distribution. For example, among females around 160 cm tall, weights ranged from 43 – 93 kg, illustrating variability in body compositions for similar heights. The broad range of participant heights (males = 165 – 194 cm, females = 153 – 178 cm) is relevant for PPG analyses where body height is recommended to be considered as a factor affecting HR estimation [50], and future work could evaluate if similar associations exist with smartwatch ECGs using this dataset.





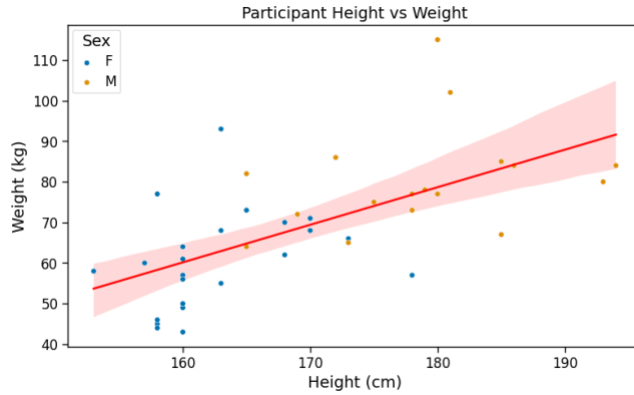


Figure 1: Participant demographics. (Top left) Stacked bar plot of age per sex. (Top right) Pie plot of self-identified race. (Bottom) Scatterplot of each participant's height and weight with fitted linear regression and 95% confidence interval (red).

### 3.3 Study Setting

Participants were scheduled for a single 1-hour visit to the Challenging Environment Assessment Laboratory (CEAL) within the Toronto Rehabilitation Institute. This controlled, indoor setting was chosen to standardize environmental conditions across sessions such as ambient lighting and sound which could influence biosignal acquisition.

### 3.4 Data Acquisition Devices

Separate devices were used to collect smartwatch signals, reference chest ECG, and BP values respectively. Since there is no common point in the system for data synchronization, Unix timestamps were generated for each sensor event and stored during collection. Smartwatch timestamps and chest ECG timestamps were recorded with nanosecond and millisecond precision respectively. Hardware details are summarized in Table 2. Smartwatch sampling rates are reported as observed at each sensor's default setting during preliminary trials; maximum smartwatch rates were not enabled because prolonged, synchronized recordings exhibited sensor instability (e.g. information loss). The default rate of the Olimex shield is 256 Hz but was set to match the sampling rate from the smartwatch ECG to 250 Hz for consistency between ECG devices.

Table 2: Summary of device details for biodata acquisition. Modalities should be considered smartwatch-derived unless indicated. A

‘—’ indicates that the category is not applicable.

Device	Signal Acquisition	Modality	Sampling rate	Data Transfer
Google Pixel Watch 2 (2022)	AFE4950, 3-axis accelerometer	ECG, PPG, ACC	250 Hz, 68 Hz, 6 Hz	Android Wireless Debugging
Olimex SHIELD-EKG-EMG, Arduino Uno	3M Red Dot ECG Electrode (2249-50)	Chest ECG	250 Hz	Micro-USB
Omron BP5000 Upper Arm Monitor	—	Cuff BP	—	Manual recording

### 3.5 Data Collection

The data collection procedure involves three main physical states: sitting, standing, and walking. BP measurements were recorded during the transition period between each of these states using the Omron digital monitor. The smartwatch was securely placed on each participants’ left wrist, while the BP cuff was placed on their upper right bicep to avoid contaminating watch signals during cuff inflation and deflation [51,52]. Three gel electrodes were placed on the chest and torso to acquire reference chest ECG data, and the presence of QRS complexes were visually verified before each physical state and BP recording. Participants were instructed to place their right index finger on the crown of the smartwatch as the researchers initiated each recording. The participants followed this procedure for both the physical state and the BP recording sessions; however, physical state sessions were 4 minutes in duration while the BP sessions were stopped after the monitor reported systolic and diastolic readings. Four minutes was chosen as the duration for physical states as multiple studies have shown that this is the minimum duration required for common frequency-domain cardiovascular metrics, such as HRV low and very low frequency power in static and non-static physical states [53,54]. Due to the aforementioned technical challenges with collecting smartwatch ECG, this duration was not extended to minimize participant burdens during the walking portion of the procedure.

During BP recordings, cuff inflation was initiated after approximately 30 seconds of biosignal recordings to establish a non-perturbed baseline. This short pre-inflation baseline was acquired due to previous findings showing that distal blood flow is modulated during cuff inflation and deflation, which could affect pulse transit time (PTT) analyses if distal PPG waveforms were impacted [55,56].

Participants were asked to avoid speaking or excessive motion during data acquisition, however, with the goal of semi-naturalistic data acquisition in mind, they were permitted to do so within reason. Additionally, smartwatch data was not accessed or visualized during data collection in real-time due to technical limitations with the device and security restrictions. The standing and walking recordings were conducted on the treadmill, Norditrack C1750, with the treadmill speed set to a moderate walking pace unique to each participant's comfortability. The maximum speed was set to 3.0 miles per hour for participant safety in accordance with our ethics approvals. To avoid variable delays and missing packets from wireless transmission [57], an offline system was designed such that the chest data was streamed serially through USB to the research laptop and the watch data was stored locally on the device. Data files, stored as CSVs, were manually extracted from the watch through Android Studio Wireless Debugging and stored on the research laptop after each participant completed the procedure. The deidentified CSVs were manually uploaded to UHN OneDrive platform after each visit. A visualization of a standard visit is presented in Figure 2.



Figure 2: Visualization of data collection procedure: seated BP → 4 minutes sitting → seated BP → standing BP → 4 minutes standing → standing BP → 4 minutes walking → standing BP. Created in BioRender. Kaetheeswaran, J. (2025) <https://BioRender.com/iubzcdu>

### 3.6 Data Organization

The raw and synchronized versions of the data have been provided as CSVs within HEART-Watch. The raw version of the data refers to the smartwatch and chest data that were recorded in their original sampling rates (refer to Table 2) and stored as separate CSVs as shown in Figure 3. The synchronized version compiles the raw files into a single CSV by zero-centering signals, applying linear interpolation to 250 Hz, and aligning via Unix timestamps. ACC signals were not zero-centered to preserve the influence of gravity. Additional synchronization was performed by estimating a constant time domain shift based on mean R-peak time differences between the smartwatch and chest ECG data and shifting the watch

signals accordingly to account for potential clock drift. The synchronized CSVs do not have any normalization or filtering techniques applied to the data to provide flexibility in processing pipelines for researchers. The following sections describe the physiological background and data-acquisition procedures for each modality.

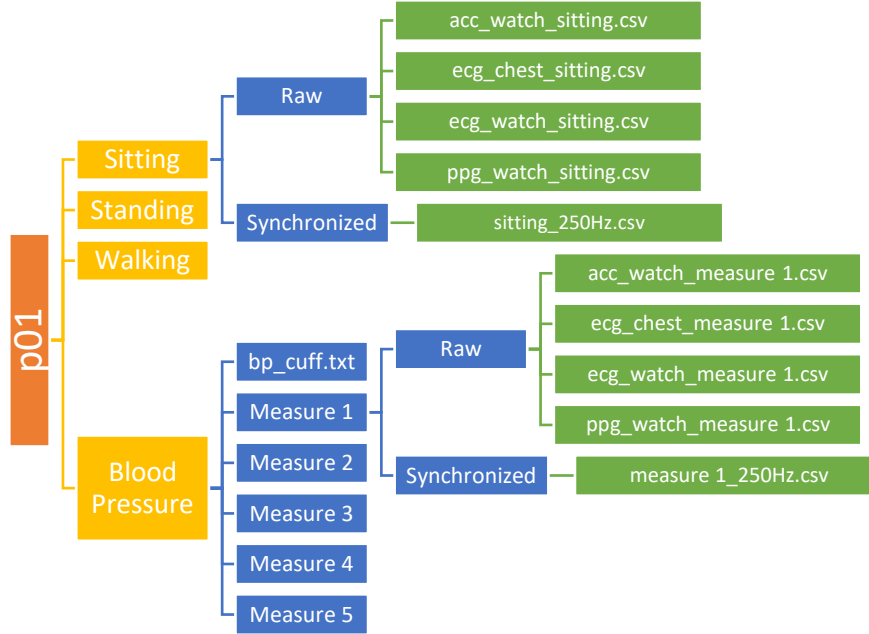


Figure 3: A visualization of the directory structure of HEART-Watch for raw and synchronized versions of the dataset for participant p01.

### 3.6.1 Chest Electrocardiogram

The reference chest ECG used in this study is a bipolar Lead I configuration consistent with Einthoven’s triangle [35]. A modified 3-electrode system was employed, with left and right electrodes placed at the respective infraclavicular fossae, and the ground electrode at the right lower rib cage [58]. The clavicle and rib cage bones were used as anatomical landmarks to guide electrode placement for consistency across participants. This electrode positioning, motivated by the work of Mason and Likar for exercise ECG [59], has been shown to produce similar Lead I data to traditional 12-lead ECG systems [60], and was chosen over limb placements to avoid excessive motion artifacts from smartwatch use or during walking. The gel electrodes, 3M Red Dot 2249-50, were chosen for their low impedance and stable performance among commercially available pregelled skin electrodes [61]. The Arduino Uno and Olimex shield were also chosen as a low-cost ECG monitoring system with strong signal amplitude due to the chain of onboard filters that increase total gain [62].

Sensor values streamed from this board represent the potential difference between the positive left electrode and the negative right electrode. A diagram illustrating the chest ECG setup is shown in Figure 4.

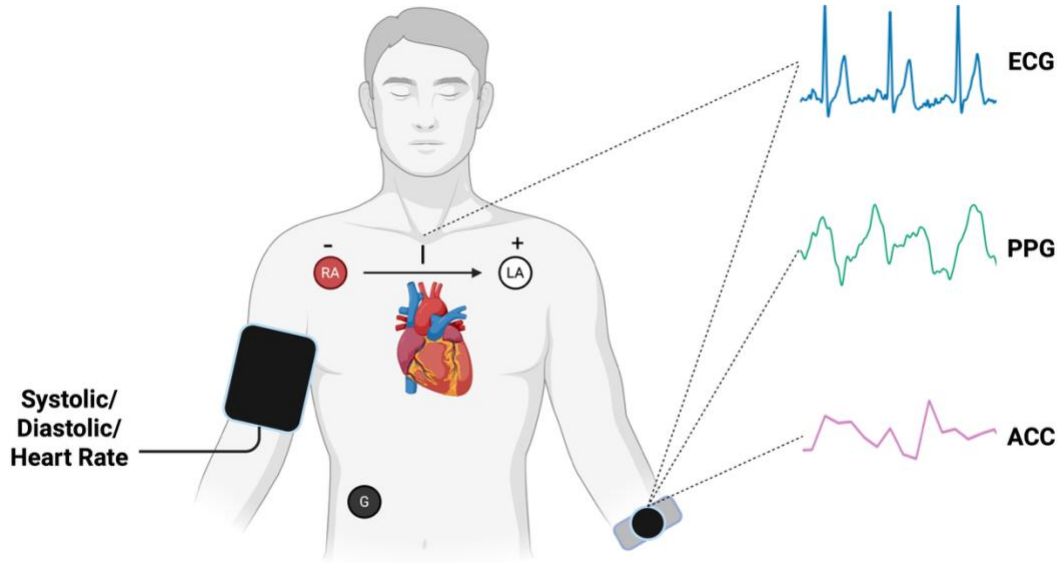


Figure 4: The data acquisition setup using a Lead I setup for chest ECG, Google Pixel Watch 2 on the left wrist for ECG, PPG, and ACC signals, and a BP cuff on the right bicep for systolic and diastolic BP measurements. Created in BioRender. Kaetheeswaran, J. (2025) <https://BioRender.com/k7cdwwt>

### 3.6.2 Smartwatch Electrocardiogram

Consumer-grade smartwatch ECGs are also bipolar Lead I recordings. The potential difference is computed between the right index finger touching the crown of the watch (negative) and the electrode on the backside of the watch contacting the wrist (positive) [35]. In this way, the Lead I signals generated from the chest ECG can be directly compared with the signals from the smartwatch ECG. ECGs are useful for providing direct insights into cardiac functions through the analysis of each PQRST complex, which is a well-defined pattern representing the depolarization and repolarization of the heart for each cardiac cycle [63]. The frequency of PQRST waves can be used to calculate HR and identify irregular durations or deflections that could represent cardiac arrhythmias such as AF [64].

### 3.6.3 Smartwatch Photoplethysmography

The smartwatch PPG sensor is typically composed of a light emitting diode (LED) and a photodetector [65]. The LED, often a green LED in wrist-based wearables, emits light through the wrist tissue, while the photodetector measures the reflected light [66]. The propagation of light energy through the wrist tissue is based on Beer-Lambert law, with the changes measured by the photodetector corresponding to changes in blood volume due to cardiac cycles [67]. In contrast to watch-based ECGs, smartwatch PPGs do not require active contact with the contralateral hand, allowing for passive, continuous monitoring from normal wear [34]. For this reason, PPG is the primary signal used for cardiovascular monitoring in wearable devices, as it can be used to estimate HR, blood oxygenation, sleep stages, and cuffless BP [6]. The AFE4950 hardware in the Google Pixel Watch 2 contains dual receiving channels: a primary PPG channel and a reference channel for motion or ambient light correction [68,69]. Our team reached out to the AFE4950 manufacturer, Texas Instruments, to request a full datasheet to identify each channel’s exact purpose but were not granted access. Based on our internal testing, the second PPG channel, denoted *ppg\_watch\_two*, should be used for pulse waveform analysis as it contains the pulsatile portion of traditional PPG signals. Therefore, it is likely that the first PPG channel, denoted *ppg\_watch\_one* is a reference channel for signal recovery, so it has been included in our published dataset but not utilized in the analyses and visualizations presented in this work.

### 3.6.4 Smartwatch Accelerometer

The electrical signals outputted from an ACC sensor are generated in response to changes in the body’s velocity per second [70]. Smartwatches are often equipped with three-axis ACC sensors that can capture dynamic movements of the device. ACC signals have been widely incorporated into existing smartwatch monitoring algorithms as it can be measured passively like PPG, and can provide useful estimations of activity metrics such as step count [6]. The utility of this modality for cardiovascular monitoring can be extended by providing valuable event-related information for filtration of motion artifacts from smartwatch ECG and PPG signals [21].

### 3.6.5 Inflatable BP Cuff

Upper arm BP monitors estimate systolic and diastolic values by applying pressure on the brachial artery and gradually deflating the cuff while measuring pressure oscillations [71]. The Omron BP5000, an FDA-registered medical device, was chosen to provide accurate readings while minimizing motion artifacts [72]. The five readouts from the digital monitor for

each participant are available in the format *systolic/diastolic/heart rate*. The first two measurements were taken while seated, while the remaining three readings are from a standing position. BP measurements could not be obtained while walking because the BP5000 device automatically terminates readings when motion artifacts are detected [72].

### 3.7 Smartwatch Application

The raw sensor values from the Google Pixel Watch 2 were collected through a custom application developed with Android Studio. The SensorManager API provided direct access to the ECG, PPG, and ACC SensorEvents which were recorded and stored in an on-device Room database along with Unix timestamps [73,74]. Kotlin coroutines were programmed to ensure that sensor database inserts were performed asynchronously on background threads without affecting ongoing sensor readouts and app performance [75].

## 4 VALIDATION

The preliminary validation of HEART-Watch is composed of (i) a visualization of synchronized signals, (ii) an assessment of signal sampling rates, (iii) an assessment of signal strength, (iv) statistical comparisons between chest and smartwatch ECG morphology, (v) an example of HR estimation techniques incorporating all smartwatch modalities, and (vi) an analysis of systolic and diastolic BP measurements.

### 4.1 Visualization of Synchronized Signals

The synchronization of the smartwatch and chest signals is shown in Figure 5 using both the raw signals as well as outputs from two common open-source Python toolboxes for biosignal processing: BioSPPy [76] and NeuroKit2 [77]. The top row presents the signals provided in the synchronized CSVs after applying min-max normalization and mean removal.

The R-wave spikes in both the chest and smartwatch ECG signals are closely aligned temporally across physical states, and the PPG oscillations are captured by both libraries' processing pipelines. Additionally, the processed PPG peaks closely follow each R-wave spike, indicating that this data is suitable for synchronicity-dependent analyses such as PTT. This visualization is intended to demonstrate the time-alignment between modalities and how commonly used scientific toolboxes can easily integrate with HEART-Watch's data.

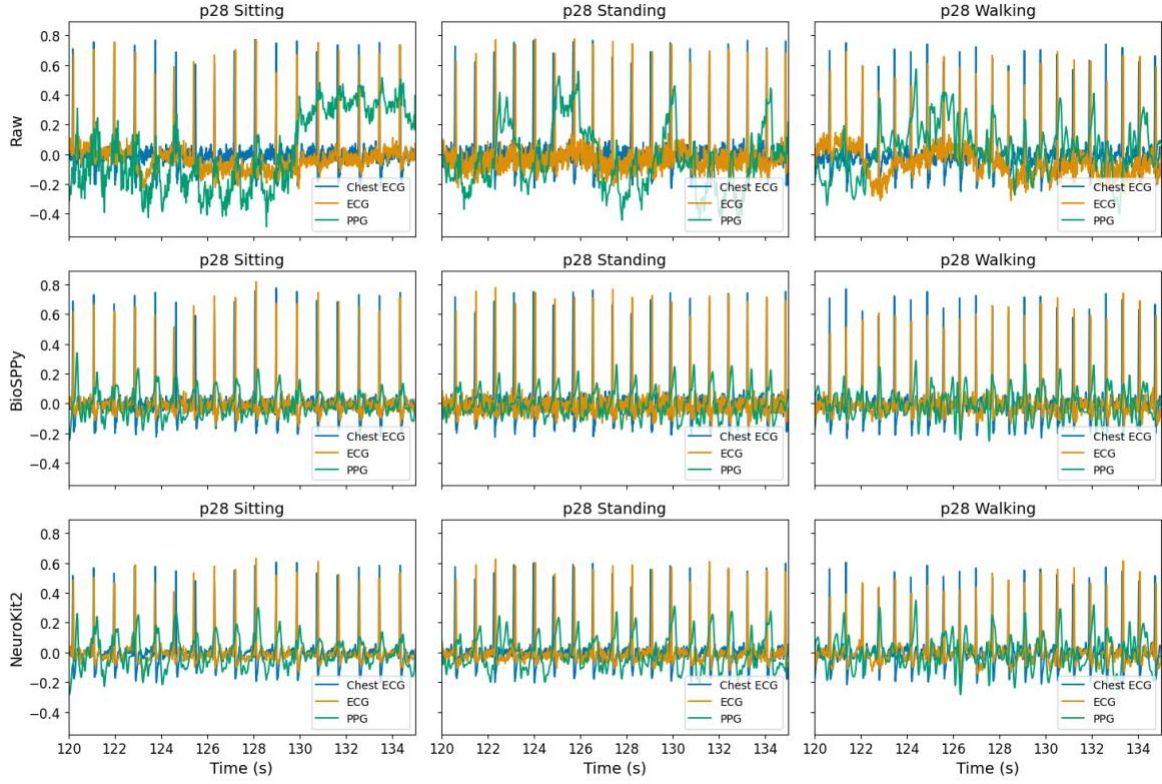


Figure 5: 15-second sample ECG and PPG waveforms from participant p28 across sitting, standing, and walking states using raw synchronized data (top row), BioSPPy (middle row) and NeuroKit2 (bottom row).

The raw ACC signals are visualized for another subject in Figure 6 across physical states. The sitting and standing states show approximately constant values across 4 minutes consistent with the expected behavior in static positions. In contrast, the walking state exhibits oscillatory waveforms across all axes due to the rhythmic upper body motion that occurs during regular gait cycles. Although participants were required to maintain wrist ECG contact while walking, it is apparent that the ACC sensors are still able to distinguish subtle upper arm swings that occurred. The clear differences in signal morphology between static and dynamic physical states highlights the value of the ACC signals for physical state-dependent filtration methods in cardiovascular analyses. Specifically, for repetitive dynamic movements such as walking, the ACC sensors can be leveraged to remove motion-related frequencies from ECG and PPG signals while preserving cardiac-related frequencies such as HR.





Figure 6: Triaxial ACC sensor values across physical states for subject p16. The walking state has notable oscillations compared to sitting and standing, which can be attributed to the slight swinging of the arms during gait cycles. Created in BioRender. Kaetheeswaran, J. (2025) <https://BioRender.com/6j7gin4>

## 4.2 Sampling Rate Assessment

Verification of sampling stability is crucial in semi-naturalistic conditions where device loads and system buffering can result in deviations [38,57]. Following the validation method presented by Park et al. [38], the mean sampling rates of the raw smartwatch and chest ECG data were computed for each activity state to verify that actual time intervals did not vary significantly during acquisitions. These time intervals were also computed during the five BP measurements. The calculated sampling rates are presented in Table 3. All biosignals were within 1Hz of their nominal rates, indicating stable sensor timing across subjects for each recording session. Minor sampling rate fluctuations are expected from sensors where internal oscillators experience small variances in frequencies [57].

Table 3: Mean sampling rates computed from raw sensor time intervals across recording sessions (SW: smartwatch).

Recording Session	Chest ECG	SW ACC	SW ECG	SW PPG
Sitting	250.13 Hz	6.27 Hz	250.93 Hz	68.43 Hz
Standing	250.14 Hz	6.27 Hz	250.95 Hz	68.44 Hz
Walking	250.11 Hz	6.27 Hz	250.96 Hz	68.44 Hz
BP Measure 1 (seated)	250.68 Hz	6.27 Hz	250.69 Hz	68.36 Hz
BP Measure 2 (seated)	250.80 Hz	6.27 Hz	250.75 Hz	68.38 Hz
BP Measure 3 (standing)	250.72 Hz	6.27 Hz	250.72 Hz	68.37 Hz
BP Measure 4 (standing)	250.71 Hz	6.27 Hz	250.74 Hz	68.38 Hz
BP Measure 5 (standing)	250.97 Hz	6.27 Hz	250.71 Hz	68.37 Hz

### 4.3 Signal Strength Assessment

The strength of the signals across physical states were evaluated using the formula presented by Park et al. [38] for classifying weak PPG and ECG signals where a segment is considered weak if the peak-to-peak values is less than 10% of the segment’s standard deviation.

$$\text{Weak PPG or ECG if: Peak-to-peak (signal)} < 0.1 * \sigma (\text{signal}) \quad (1)$$

The 4-minute ECG recordings were first min-max normalized and zero-centered, before being segmented into 30-second windows to calculate standard deviation. This window length was chosen because it is the standard smartwatch ECG duration for analyses [33]. The PPG recordings followed the same preprocessing with the addition of NeuroKit2 cleaning to remove baseline wander. The 30-second windows were segmented into 2-second non-overlapping windows to compute peak-to-peak values. Signals were considered weak if any of these 2-second windows matched the weak signal definition. Windows with lead fall-offs or signal saturation were considered invalid signals, and defined as windows where peak-to-peak values were zero as suggested by Liu et al. [78]. Windows were also classified as invalid if they contained any not a number (NaN) values. The same ACC signal criteria used by Park et al. [38] was implemented here, where

windows with ACC vector magnitudes greater than an upper bound were considered invalid. The upper bound was set to 1.5g after reviewing the findings of Strackiewicz et al. which show that ACC values during walking are usually below this value [79]. ACC measurements, recorded in  $m/s^2$ , were converted to gravitational units before evaluating validity.

An additional assessment for ECG signals was derived by comparing each 30-second segment's peak-to-peak value with the ones derived from its internal 2-second windows. A 2-second ECG window was labelled weak if the peak-to-peak value was less than 50% of the 30-second segment's peak-to-peak reference. To avoid overclassifying segments as weak, a 30-second segment was classified as weak if more than 50% of its 2-second windows were weak. This additional check was necessary for addressing ECG segments with both strong and weak QRS complexes, such as in the example provided in Figure 7.

The results of this assessment are presented in Table 4. The smartwatch ECG was the only modality that contained weak or invalid segments, and it was expected due to the dependence of signal quality on prolonged finger contact. The sitting and standing states have similar rates of 5.31% and 5.20% respectively as these are static positions. The walking state showed the highest level of weak or invalid signals at 12.50%, illustrating the difficulties of recording prolonged smartwatch ECGs during physical activity. The benefit of the offline data transmission system is also highlighted by zero NaN signal values being detected across modalities and physical states.

Table 4: Percentage of weak or invalid 30-second segments across modalities and physical states (SW: smartwatch).

Physical State	Chest ECG	SW ACC	SW ECG	SW PPG
Sitting	0.00 %	0.00 %	5.31 %	0.00 %
Standing	0.00 %	0.00 %	5.00 %	0.00 %
Walking	0.00 %	0.00 %	12.50 %	0.00 %

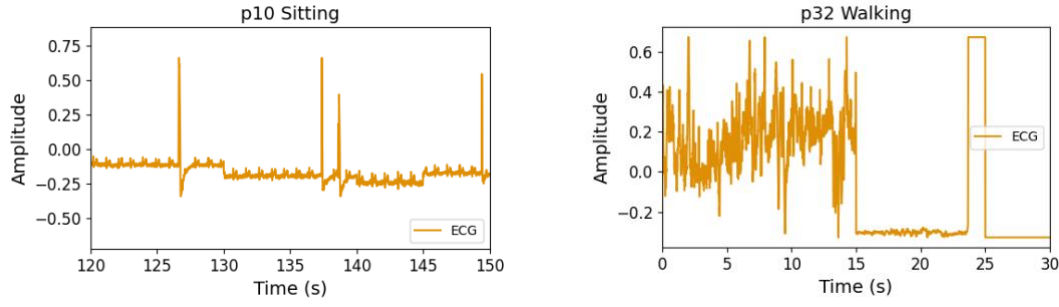


Figure 7: 30-second smartwatch ECG example of a window with strong and weak QRS amplitudes (left), and a window with signal saturation and/or lead fall-off issues leading to a square wave morphology (right).

#### 4.4 Electrocardiogram Morphology Comparison - QRS and PR Intervals

To compare the signal morphology of the single-lead smartwatch ECG with the chest ECG, statistical analyses on the QRS and PR intervals were performed. The QRS interval is defined as the duration between the onset and offset of the QRS complex, and used as a predictor for cardiovascular mortality [80,81]. The PR interval is defined as the duration between the onset of the P-wave and the onset of the QRS complex, and is also a commonly-used biomarker for cardiovascular health [82,83].

Automatic ECG delineation was conducted using the Peak Prominence ECG Delineator, which applies physiological constraints to identify fiducial points with high temporal accuracy [84]. Following the methodology of Van Der Zande et al. [33], mean durations were calculated for each participant and activity state, and Bland-Altman plots were generated to compare biases and limits of agreement (LoAs) between the smartwatch ECG and chest ECG (see Figure 8). A paired  $t$ -test was conducted to evaluate the statistical significance of these biases across states, where  $p < 0.05$  was considered statistically significant.

Minimal bias was observed for QRS intervals across all three conditions (sitting: +1.51 ms, standing: +1.04 ms, walking: +1.93 ms) in addition to narrow LoAs. During standing, the QRS bias was not statistically significant ( $p = 0.09$ ). Although the sitting and walking state biases are statistically significant ( $p < 0.05$ ), they have low magnitudes that are 1-2% of normal QRS intervals (80-100 ms). In contrast, smartwatch PR intervals showed a strong bias towards overestimation across physical states (sitting: +10.09 ms, standing: +13.22 ms, walking: +17.71 ms) with wide LoAs. These biases were statistically significant across all states ( $p < 0.001$ ), suggesting that there is a consistent overestimation

of PR intervals by the smartwatch ECG. Since this bias was not observed for QRS interval measurements, it is possible that P-waves are detected incorrectly compared to the QRS complexes due to attenuation of these points, aligning with previous findings on the limitations of Lead I smartwatch ECGs [85,86].

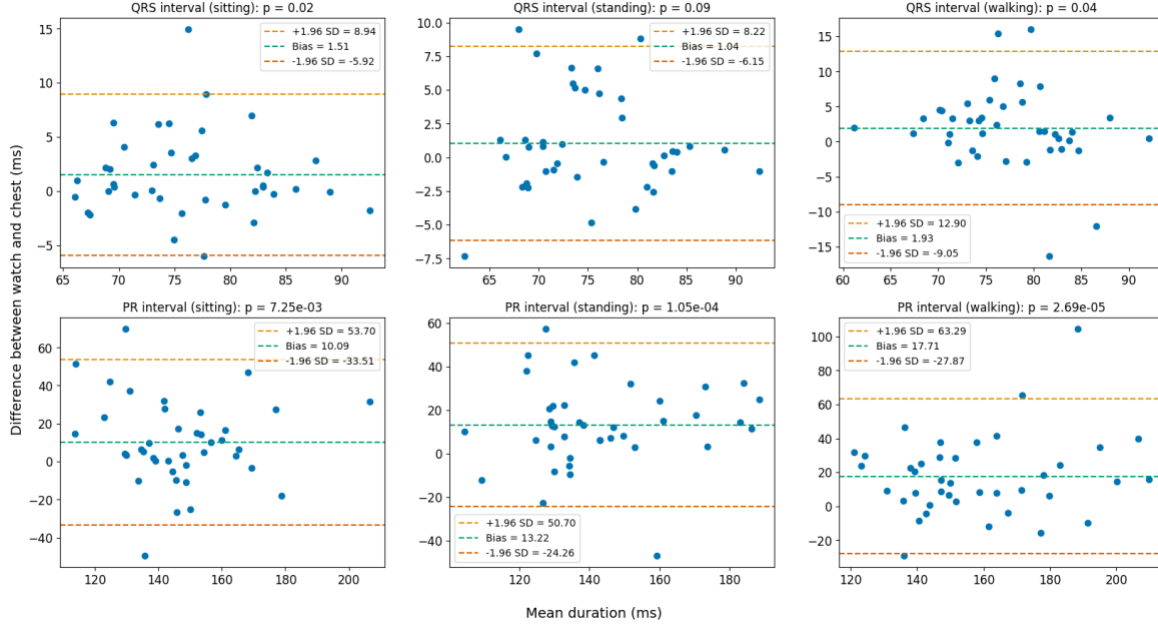


Figure 8: Bland-Altman plots for QRS and PR intervals across the main physical states with dashed lines for the bias (green), upper limit of agreement (orange), and lower limit of agreement (red).

#### 4.5 Heart Rate Analysis

The synchronization of the smartwatch signals enables applications, such as long-term HR monitoring, across daily activities. Figure 9 illustrates how instantaneous heart rate (IHR) can be computed from chest ECG, smartwatch ECG, and smartwatch PPG during sitting, standing and walking states. IHR is defined as 60 seconds divided by the duration, in seconds, between successive ECG R-peaks to yield a value in beats-per-minute (BPM) [87,88]. Smartwatch HR values were estimated using the adaptive notch-filtration approach by Zheng et al. [89] which identifies three candidate frequencies for notch filtering based on the raw ACC signals. These candidate frequencies are attributed to motion oscillations, as shown in Figure 6, unless there is overlap with ECG or PPG frequency peaks. Here, IHR was computed with a 10-second sliding window, a 1-second step size, and a tolerance of 10 beats per minute (BPM).

Although the adaptive notch-filtration approach was originally designed for PPG signals during physical activity, the implementation also performs well with smartwatch ECG signals. Notably, the choice of ACC axis for this approach appears to have significant effects on the smartwatch IHRs relative to the chest ECG IHRs. Future analyses may benefit from examining how careful selection or fusion of ACC axes can enhance filtration techniques across the physical states for each participant or demographic group. This example highlights the value of synchronized ACC signals in addition to the wrist-based ECG and PPG, demonstrating how these modalities can be combined to compare estimation techniques for continuous monitoring.

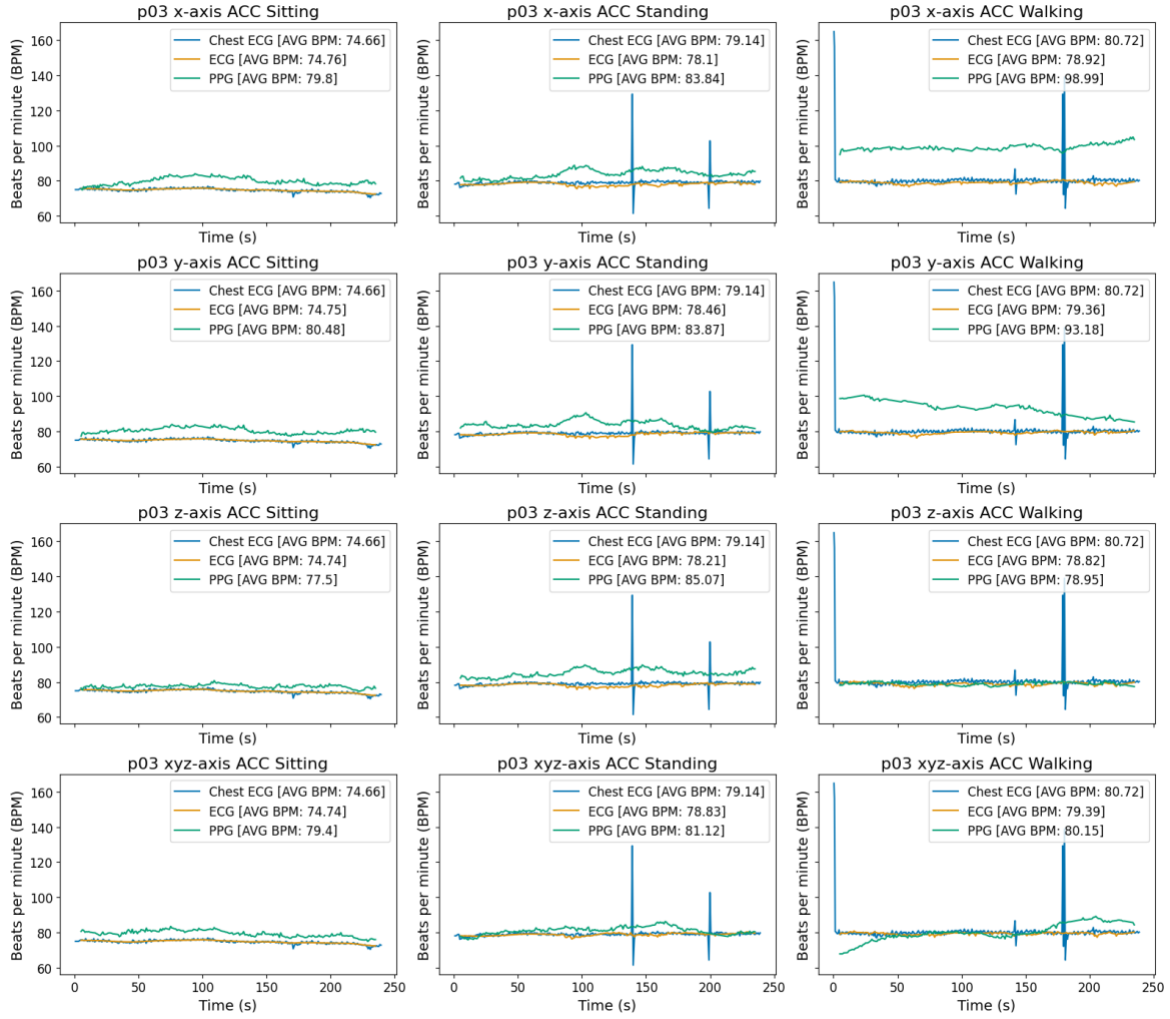


Figure 9: IHR estimation plots for participant p03 across physical states using different ACC axes for adaptive notch-filtration on the smartwatch ECG and PPG signals.

#### 4.6 Blood Pressure Measurements

Upper arm BP measurements were recorded for each participant, and boxplots along with descriptive statistics are provided in Figure 10 and Table 5 respectively. Males exhibited higher median systolic and diastolic values than females, although several female outliers with high systolic and diastolic pressures were observed. Females also demonstrated a tighter distribution of diastolic pressures compared to the males. These differences highlight the importance of including diverse cohorts when constructing cardiac datasets to capture biomarker variability. These BP recordings can be analyzed

with the synchronized chest ECG and smartwatch ECG, PPG, and ACC collected before and during cuff inflation. An application of this would be for cuffless BP estimation, which usually pairs distal PPG waveforms with chest ECG R-peaks to compute PTT [90]. While existing PTT-based works with smartwatches have employed wrist-based PPG methods, the HEART-Watch dataset is unique in offering simultaneous wrist-based ECG and ACC signals in addition to detailed demographic information. This combination may provide researchers with new avenues for continuous BP estimation techniques using consumer-grade smartwatches by incorporating these new modalities.

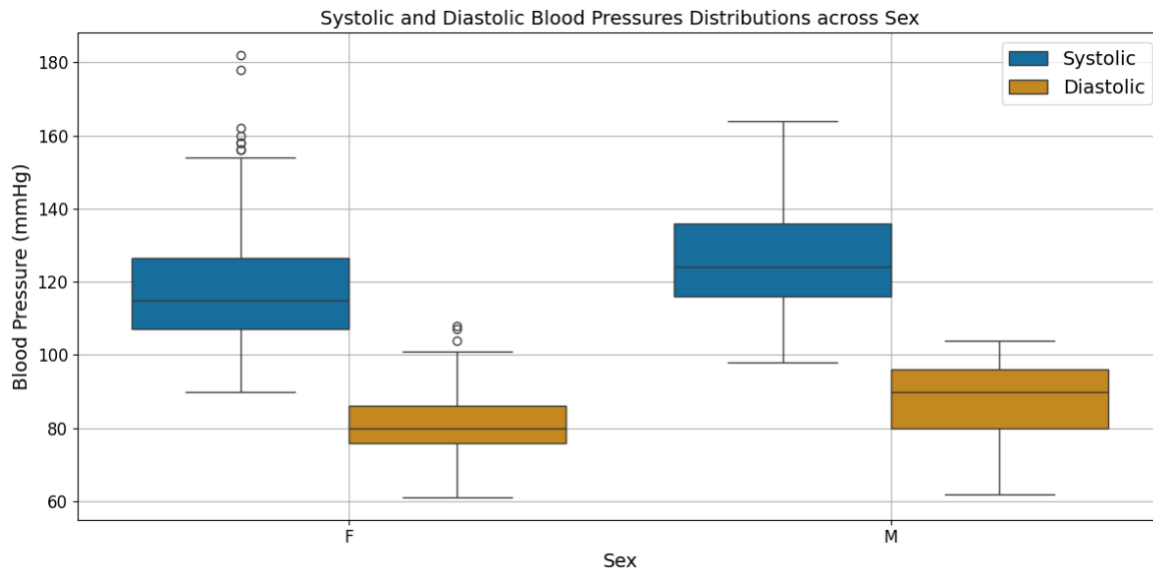


Figure 10: Boxplots to visualize distribution of systolic and diastolic BP cuff readings between females and males.

Table 5: Summary of boxplot statistics for systolic and diastolic BP readings per sex.

Sex	Number of observations	BP Type	Mean (mmHg)	Q1 (mmHg)	Q2/Median (mmHg)	Q3 (mmHg)
Female	115	Systolic/Diastolic	120/81	107/76	115/80	127/86
Male	85	Systolic/Diastolic	127/87	116/80	124/90	136/96



## 5 DISCUSSION

This study was conducted in a semi-naturalistic environment that relied on participant compliance for extended periods of time. During sitting and standing phases, participants were permitted reasonable movement rather than being strictly static across 4 minutes, which may have introduced noise into the acquired signals. Participants also showed varying levels of compatibility with both the chest ECG system and the smartwatch for achieving high-quality waveforms.

During chest ECG calibrations before each recording, it was visually observed that females often had higher levels of noise present in their signals, a finding that aligns with previous research suggesting that breast tissue may interfere with signal quality [39]. Similarly, our team visually observed degradations in chest ECG quality, specifically for identifying QRS complexes, when participants had rounded shoulders while collecting smartwatch ECGs. These artifacts are associated with changes in the heart's orientation within the chest cavity, and deviations from traditional supine recordings have been linked to significant variations in ECG morphology [91]. As a result, reference chest ECG signals likely contain noise or motion artifacts due to these conditions.

Additionally, participants were instructed to maintain contact with the smartwatch using their right index finger for smartwatch ECGs. It is likely that participants did not maintain optimal contact for the entire duration of the recordings, leading to saturation or motion artifacts such as the examples presented in Figure 7. All recordings are included as these phenomena are encouraged as robustness concepts for machine learning in healthcare [31]. Similarly, the wrist-based PPG waveforms are susceptible to artifacts from skin tone, wrist contact, skin perfusion, and motion artifacts [21]. The diverse cohort of participants and physical states will likely influence PPG signal quality, and future analyses may benefit from incorporating the first PPG channel into their algorithms for corrections using this reference channel.

Finally, the use of separate devices and system clocks introduced the risk of clock drifts and jitters, which are common issues in clinical environments [21,57]. To minimize these concerns, smartwatch clocks were manually synchronized with Coordinated Universal Time before each session and researchers avoided recording with watch battery levels below 50% to limit system lags or sensor instability.

## 6 CONCLUSION

Wearable technology is rapidly advancing as the market for personalized healthcare grows on a global scale. Consumer-grade smartwatches, in particular, provide accessible and affordable continuous health monitoring to the general public.

However, the development of robust signal processing and AI algorithms requires training and validation with realistic, long-form raw sensor data collected across diverse participants. HEART-Watch addresses this need by providing synchronized smartwatch signals – including PPG, ACC, and prolonged ECG recordings – alongside chest ECG across common physical states. In addition, BP cuff values and corresponding biosignals are available as an additional benchmark for cardiovascular research. The inclusion of participants with varied race, age, sex, and body types is intended to support fairness assessments for solutions that can generalize across populations. Validation tests confirmed consistent sampling rates and high-quality signals suitable for cardiovascular analyses.

Although the semi-naturalistic nature of this dataset may introduce artifacts that can degrade signal quality, it is also a reflection of the realistic challenges of wearable sensors. Rather than excluding such data, it can be leveraged to design and validate algorithms that are resilient to these variations. In this way, HEART-Watch offers the research community a resource for advancing the development of consumer-grade smartwatch algorithms that are both robust and equitable.

## 7 DATASET AND CODE AVAILABILITY

The HEART-Watch dataset is maintained through the UHN OneDrive platform. Researchers who are interested in obtaining this dataset for research purposes should contact the principal investigator at [shehroz.khan@uhn.ca](mailto:shehroz.khan@uhn.ca). Data will be made available to researchers who submit details of a study plan and sign the data-use agreement to maintain participant confidentiality and ensure compliance with ethical standards. The Jupyter Notebook code for data organization and validation will be shared alongside the HEART-Watch dataset following successful requests. An outline of the available scripts is described here:

- (i) *synchronize.ipynb* – Compiles raw CSVs into a single temporally synchronized CSV for each subject with all modalities at 250 Hz following the process described in section 3.6.
- (ii) *demographics.ipynb* – Generates bar, pie, and scatter plots for participant demographics as shown in Figure 1. Also generates boxplots in Figure 10 to visualize blood pressure distributions across sex.
- (iii) *visualize.ipynb* – Generates subject-specific time-series visualizations of ECG, PPG, and ACC signals as shown in Figure 5 and Figure 6.
- (iv) *sampling\_rate.ipynb* – Computes mean sampling rates of ECG, PPG, and ACC signals across all participants and physical states as shown in Table 3.

- (v) *signal\_strength.ipynb* – Computes percentage of 30-second segments containing weak ECG, PPG and ACC signals across all participants and physical states as shown in Table 4.
- (vi) *ecg\_morphology.ipynb* – Computes QRS and PR intervals using the chest and smartwatch ECGs and formats the results into the Bland-Altman plots shown in Figure 8.3.63.6
- (vii) *heart\_rate.ipynb* – Calculates heart rate for a subject from ECG and PPG signals after adaptive filtration is applied using the ACC signal and generates plots for each ACC axis as shown in Figure 9.3.6

## ACKNOWLEDGMENTS

This work is funded through the Natural Sciences and Engineering Research Council of Canada (NSERC) Alliance Advantage (Grant #: 110\_2023\_2024\_Q4\_446). The authors would like to thank CEAL for their cooperation during the data collection process.

## REFERENCES

1. Chong B, Jayabaskaran J, Jauhari SM, Chan SP, Goh R, Kueh MTW, et al. Global burden of cardiovascular diseases: projections from 2025 to 2050. *Eur J Prev Cardiol*. 2025 Aug 25;32(11):1001–15.
2. Vaduganathan M, Mensah GA, Turco JV, Fuster V, Roth GA. The Global Burden of Cardiovascular Diseases and Risk. *J Am Coll Cardiol*. 2022 Dec;80(25):2361–71.
3. Lee J, Kim D, Ryoo HY, Shin BS. Sustainable Wearables: Wearable Technology for Enhancing the Quality of Human Life. *Sustainability*. 2016 May 11;8(5):466.
4. Sadiq I, Ijaz A, Imran A. Wrist-Worn Devices for Remote Monitoring of Cardiovascular Disease: A Survey. *IEEE Access*. 2025;13:151111–36.
5. Steinhubl SR, Muse ED, Topol EJ. The emerging field of mobile health. *Sci Transl Med [Internet]*. 2015 Apr 15 [cited 2025 Sept 19];7(283). Available from: <https://www.science.org/doi/10.1126/scitranslmed.aaa3487>
6. Bayoumy K, Gaber M, Elshafeey A, Mhaimeed O, Dineen EH, Marvel FA, et al. Smart wearable devices in cardiovascular care: where we are and how to move forward. *Nat Rev Cardiol*. 2021 Aug;18(8):581–99.
7. Hughes A, Shandhi MMH, Master H, Dunn J, Brittain E. Wearable Devices in Cardiovascular Medicine. *Circ Res*. 2023 Mar 3;132(5):652–70.
8. Global Market Insights. Smartwatch Market Size, Share and Industry Analysis [Internet]. 2025. Available from: <https://www.gminsights.com/industry-analysis/smartwatch-market>
9. Liao Y, Thompson C, Peterson S, Mandrola J, Beg MS. The Future of Wearable Technologies and Remote Monitoring in Health Care. *Am Soc Clin Oncol Educ Book*. 2019 May;(39):115–21.
10. Manninger M, Zweiker D, Svennberg E, Chatzikyriakou S, Pavlovic N, Zaman JAB, et al. Current perspectives on wearable rhythm recordings for clinical decision-making: the wEHRables 2 survey. *EP Eur*. 2021 July 18;23(7):1106–13.
11. Alugubelli N, Abuissa H, Roka A. Wearable Devices for Remote Monitoring of Heart Rate and Heart Rate Variability—What We Know and What Is Coming. *Sensors*. 2022 Nov 17;22(22):8903.
12. Friedman P, Lopez-Jimenez F, Nishimura R, Attia Z. Artificial Intelligence and Wearables in Cardiology—Promise and Peril. *Am J Cardiol*. 2022;183:127–35.

13. Rising CJ, Gaysynsky A, Blake KD, Jensen RE, Oh A. Willingness to Share Data From Wearable Health and Activity Trackers: Analysis of the 2019 Health Information National Trends Survey Data. *JMIR MHealth UHealth*. 2021 Dec 13;9(12):e29190.
14. Francisco A, Pascoal C, Lamborne P, Morais H, Gonçalves M. Wearables and Atrial Fibrillation: Advances in Detection, Clinical Impact, Ethical Concerns, and Future Perspectives. *Cureus*. 2025;17(1).
15. Mühlen JM, Stang J, Lykke Skovgaard E, Judice PB, Molina-Garcia P, Johnston W, et al. Recommendations for determining the validity of consumer wearable heart rate devices: expert statement and checklist of the INTERLIVE Network. *Br J Sports Med*. 2021 July;55(14):767–79.
16. Shcherbina A, Mattsson C, Waggott D, Salisbury H, Christle J, Hastie T, et al. Accuracy in Wrist-Worn, Sensor-Based Measurements of Heart Rate and Energy Expenditure in a Diverse Cohort. *J Pers Med*. 2017 May 24;7(2):3.
17. Mannhart D, Lischer M, Knecht S, Du Fay De Lavallaz J, Strebel I, Serban T, et al. Clinical Validation of 5 Direct-to-Consumer Wearable Smart Devices to Detect Atrial Fibrillation. *JACC Clin Electrophysiol*. 2023 Feb;9(2):232–42.
18. Browning S. 510(k) summary: Apple Inc. — Hypertension Notification Feature (K250507) [Internet]. U.S. Food & Drug Administration; 2025. Available from: [https://www.accessdata.fda.gov/cdrh\\_docs/pdf25/K250507.pdf](https://www.accessdata.fda.gov/cdrh_docs/pdf25/K250507.pdf)
19. Love CJ, Lampert J, Huneycutt D, Musat DL, Shah M, Enciso JES, et al. Clinical implementation of an AI-enabled ECG for hypertrophic cardiomyopathy detection. *Heart*. 2025 Apr 16;heartjnl-2024-325608.
20. Alizadeh Meghraz M, Tian Y, Mahnam A, Bhattachan P, Eskandarian L, Taghizadeh Kakhki S, et al. Multichannel ECG recording from waist using textile sensors. *Biomed Eng OnLine*. 2020 Dec;19(1):48.
21. Bent B, Goldstein BA, Kibbe WA, Dunn JP. Investigating sources of inaccuracy in wearable optical heart rate sensors. *Npj Digit Med*. 2020 Feb 10;3(1):18.
22. Icenhower A, Murphy C, Brooks AK, Irby M, N'dah K, Robison J, et al. Investigating the accuracy of Garmin PPG sensors on differing skin types based on the Fitzpatrick scale: cross-sectional comparison study. *Front Digit Health*. 2025;7.
23. Lubitz SA, Faranesh AZ, Selvaggi C, Atlas SJ, McManus DD, Singer DE, et al. Detection of Atrial Fibrillation in a Large Population Using Wearable Devices: The Fitbit Heart Study. *Circulation*. 2022 Nov 8;146(19):1415–24.
24. Perez MV, Mahaffey KW, Hedlin H, Rumsfeld JS, Garcia A, Ferris T, et al. Large-Scale Assessment of a Smartwatch to Identify Atrial Fibrillation. *N Engl J Med*. 2019 Nov 14;381(20):1909–17.
25. Silva FB, Uribe LFS, Cepeda FX, Alquati VFS, Guimarães JPS, Silva YGA, et al. Sleep staging algorithm based on smartwatch sensors for healthy and sleep apnea populations. *Sleep Med*. 2024 July;119:535–48.
26. Hung SH, Serwa K, Rosenthal G, Eng JJ. Validity of heart rate measurements in wrist-based monitors across skin tones during exercise. Sbrollini A, editor. *PLOS ONE*. 2025 Feb 10;20(2):e0318724.
27. Abedi A, Verma A, Jain D, Kaetheeswaran J, Chui C, Lankarany M, et al. Artificial Intelligence-driven Real-time Monitoring of Cardiovascular Conditions with Wearable Devices: A Scoping Review (Preprint). *JMIR MHealth UHealth*. 2025;
28. Nelson BW, Low CA, Jacobson N, Areán P, Torous J, Allen NB. Guidelines for wrist-worn consumer wearable assessment of heart rate in biobehavioral research. *Npj Digit Med*. 2020 June 26;3(1):90.
29. Tian Y, Abdizadeh M, Mahnam A, Bhattachan P, Meghraz MA, Eskandarian L, et al. Modeling and Reconstructing Textile Sensor Noise: Implications for Wearable Technology. In: 2020 42nd Annual International Conference of the IEEE Engineering in Medicine & Biology Society (EMBC) [Internet]. Montreal, QC, Canada: IEEE; 2020 [cited 2025 Oct 29]. p. 4563–6. Available from: <https://ieeexplore.ieee.org/document/9176393/>
30. de Zambotti M, Goldstein C, Cook J, Menghini L, Altini M, Cheng P, et al. State of the science and recommendations for using wearable technology in sleep and circadian research. *Sleep*. 2024;47(4).
31. Balendran A, Beji C, Bouvier F, Khalifa O, Evgeniou T, Ravaud P, et al. A scoping review of robustness concepts for machine learning in healthcare. *Npj Digit Med*. 2025 Jan 17;8(1):38.
32. Jaeger KM, Nissen M, Flaucher M, Graf L, Joanidopoulos J, Anneken L, et al. Systematic Comparison of ECG Delineation Algorithm Performance on Smartwatch Data. *IEEE Access*. 2024;12:160794–804.
33. Van Der Zande J, Strik M, Dubois R, Ploux S, Alrub SA, Caillol T, et al. Using a Smartwatch to Record Precordial Electrocardiograms: A Validation Study. *Sensors*. 2023 Feb 25;23(5):2555.

34. Hwang S, Seo J, Jebelli H, Lee S. Feasibility analysis of heart rate monitoring of construction workers using a photoplethysmography (PPG) sensor embedded in a wristband-type activity tracker. *Autom Constr.* 2016 Nov;71:372–81.
35. Samol A, Bischof K, Luani B, Pascut D, Wiemer M, Kaese S. Single-Lead ECG Recordings Including Einthoven and Wilson Leads by a Smartwatch: A New Era of Patient Directed Early ECG Differential Diagnosis of Cardiac Diseases? *Sensors.* 2019;19(20):4377.
36. Bent B, Dunn J. BigIdeasLab\_STEP: Heart rate measurements captured by smartwatches for differing skin tones (version 1.0). 2021.
37. Biswas N, Ashili S. Smartwatch heart rate data. 2023.
38. Park S, Zheng D, Lee U. A PPG Signal Dataset Collected in Semi-Naturalistic Settings Using Galaxy Watch. *Sci Data.* 2025 May 28;12(1):892.
39. Baigutanova A, Park S, Constantinides M, Lee SW, Quercia D, Cha M. In-situ wearable-based dataset of continuous heart rate variability monitoring accompanied by sleep diaries [Internet]. figshare; 2025 [cited 2025 Sept 18]. p. 19793309660 Bytes. Available from: [https://springernature.figshare.com/articles/dataset/In-situ\\_wearable-based\\_dataset\\_of\\_continuous\\_heart\\_rate\\_variability\\_monitoring\\_accompanied\\_by\\_sleep\\_diaries/28509740/1](https://springernature.figshare.com/articles/dataset/In-situ_wearable-based_dataset_of_continuous_heart_rate_variability_monitoring_accompanied_by_sleep_diaries/28509740/1)
40. Baigutanova A, Park S, Constantinides M, Lee SW, Quercia D, Cha M. A continuous real-world dataset comprising wearable-based heart rate variability alongside sleep diaries. *Sci Data.* 2025 Aug 23;12(1):1474.
41. Ravanelli N, Lin W, Richard M, Paquette S, KarLee Lefebvre, Brough A. Data and code for assessing the agreement of the Bangle.js2 during in-lab and 24h free-living conditions for measuring steps and heart rate. 2025 [cited 2025 Oct 3]; Available from: <https://osf.io/8mzg5/>
42. Ravanelli N, Lefebvre K, Brough A, Paquette S, Lin W. Validation of an Open-Source Smartwatch for Continuous Monitoring of Physical Activity and Heart Rate in Adults. *Sensors.* 2025;25(9):2926.
43. Reece JD, Bunn JA, Choi M, Navalta JW. Assessing Heart Rate Using Consumer Technology Association Standards. *Technologies.* 2021 June 30;9(3):46.
44. Bentov I, Reed MJ. The effect of aging on the cutaneous microvasculature. *Microvasc Res.* 2015 July;100:25–31.
45. Mannhart D, Lischer M, Knecht S, Du Fay De Lavallaz J, Strebel I, Serban T, et al. Clinical Validation of 5 Direct-to-Consumer Wearable Smart Devices to Detect Atrial Fibrillation. *JACC Clin Electrophysiol.* 2023 Feb;9(2):232–42.
46. Sarhaddi F, Kazemi K, Azimi I, Cao R, Niela-Vilén H, Axelin A, et al. A comprehensive accuracy assessment of Samsung smartwatch heart rate and heart rate variability. Mian Qaisar S, editor. *PLOS ONE.* 2022 Dec 8;17(12):e0268361.
47. Jaiswal P, Sahu NK, Lone HR. Comparative Assessment of Smartwatch Photoplethysmography Accuracy. *IEEE Sens Lett.* 2024 Jan;8(1):1–4.
48. Park S, Zheng D, Lee U. GalaxyPPG: A PPG Signal Dataset Collected in Semi-Naturalistic Settings Using Galaxy Watch [Internet]. Zenodo; 2025 [cited 2025 Sept 18]. Available from: <https://zenodo.org/doi/10.5281/zenodo.14635822>
49. KITE. Research study recruitment [Internet]. 2025. Available from: <https://kite-uhn.com/recruit>
50. Mühlen JM, Stang J, Lykke Skovgaard E, Judice PB, Molina-Garcia P, Johnston W, et al. Recommendations for determining the validity of consumer wearable heart rate devices: expert statement and checklist of the INTERLIVE Network. *Br J Sports Med.* 2021 July;55(14):767–79.
51. Ganti VG, Carek AM, Nevius BN, Heller JA, Etemadi M, Inan OT. Wearable Cuff-Less Blood Pressure Estimation at Home via Pulse Transit Time. *IEEE J Biomed Health Inform.* 2021 June;25(6):1926–37.
52. He J, Ou J, He A, Shu L, Liu T, Qu R, et al. A new approach for daily life Blood-Pressure estimation using smart watch. *Biomed Signal Process Control.* 2022 May;75:103616.
53. Bourdillon N, Schmitt L, Yazdani S, Vesin JM, Millet GP. Minimal Window Duration for Accurate HRV Recording in Athletes. *Front Neurosci.* 2017 Aug 10;11:456.
54. Kim JW, Seok HS, Shin H. Is Ultra-Short-Term Heart Rate Variability Valid in Non-static Conditions? *Front Physiol.* 2021 Mar 30;12:596060.

55. Bogatu LI, Turco S, Mischi M, Schmitt L, Woerlee P, Bresch E, et al. Modulation of Pulse Propagation and Blood Flow via Cuff Inflation—New Distal Insights. *Sensors*. 2021 Aug 19;21(16):5593.
56. Xie C, Wan C, Wang Y, Song J, Wu D, Li Y. Effects of Pulse Transit Time and Pulse Arrival Time on Cuff-less Blood Pressure Estimation: A Comparison Study with Multiple Experimental Interventions. In: 2023 45th Annual International Conference of the IEEE Engineering in Medicine & Biology Society (EMBC) [Internet]. Sydney, Australia: IEEE; 2023 [cited 2025 Mar 20]. p. 1–4. Available from: <https://ieeexplore.ieee.org/document/10340548/>
57. Goodwin AJ, Eytan D, Dixon W, Goodfellow SD, Doherty Z, Greer RW, et al. Timing errors and temporal uncertainty in clinical databases—A narrative review. *Front Digit Health*. 2022 Aug 18;4:932599.
58. Macfarlane PW. Lead Systems. In: *Comprehensive Electrocardiology*. Springer, London; 2010.
59. Mason RE, Likar I. A new system of multiple-lead exercise electrocardiography. *Am Heart J*. 1966;71:196–205.
60. Hassan S. Advances in AI-enabled Wearable Systems. *Adv Intell Syst*. 2023;
61. Man TTC, Yip YWY, Cheung FKF, Lee WS, Pang CP, Brelén ME. Evaluation of Electrical Performance and Properties of Electroretinography Electrodes. *Transl Vis Sci Technol*. 2020;9(7):45.
62. Güttler J, Georgoulas C, Linner T, Bock T. Evaluation of low cost capacitive ECG prototypes: A hardware/software approach. In 2016. p. 129–34.
63. Chapter 3, Conquering the ECG. In: *Cardiology explained* [Internet]. London ; Chicago: Remedica; 2004. (Remedica explained series). Available from: <https://www.ncbi.nlm.nih.gov/books/NBK2214/>
64. Abu-Alrub S, Strik M, Ramirez FD, Moussaoui N, Racine HP, Marchand H, et al. Smartwatch Electrocardiograms for Automated and Manual Diagnosis of Atrial Fibrillation: A Comparative Analysis of Three Models. *Front Cardiovasc Med*. 2022 Feb 4;9:836375.
65. Ghamari M. A review on wearable photoplethysmography sensors and their potential future applications in health care. *Int J Biosens Bioelectron*. 2018;4(4).
66. Charlton PH, Allen J, Bailón R, Baker S, Behar JA, Chen F, et al. The 2023 wearable photoplethysmography roadmap. *Physiol Meas*. 2023;44(11):111001.
67. Rybynok VO, Kyriacou PA. Beer-lambert law along non-linear mean light pathways for the rational analysis of Photoplethysmography. *J Phys Conf Ser*. 2010 July 1;238:012061.
68. Pandey RK, Chao PCP. A Dual-Channel PPG Readout System With Motion-Tolerant Adaptability for OLED-OPD Sensors. *IEEE Trans Biomed Circuits Syst*. 2022 Feb;16(1):36–51.
69. Texas Instruments. AFE4950 Integrated Analog Front-End [Internet]. 2025. Available from: <https://www.ti.com/product/AFE4950#product-details>
70. Minh NC, Dao TH, Tran DN, Huy NQ, Thu NT, Tran DT. Evaluation of Smartphone and Smartwatch Accelerometer Data in Activity Classification. In IEEE; 2021. p. 33–8.
71. Pilz N, Picone DS, Patzak A, Opatz OS, Lindner T, Fessler L, et al. Cuff-based blood pressure measurement: challenges and solutions. *Blood Press*. 2024 Dec 31;33(1):2402368.
72. Iron Upper Arm Blood Pressure Monitor [Internet]. OMRON Healthcare. 2025. Available from: <https://omronhealthcare.com/en-ca/products/iron-upper-arm-blood-pressure-monitor-bp5000>
73. Android Developers. SensorManager | API reference [Internet]. 2025. Available from: <https://developer.android.com/reference/android/hardware/SensorManager>
74. Android Developers. Room Database Training [Internet]. 2025. Available from: <https://developer.android.com/training/data-storage/room>
75. Android Developers. Kotlin Coroutines [Internet]. 2025. Available from: <https://developer.android.com/kotlin/coroutines>
76. Bota P, Silva R, Carreiras C, Fred A, Da Silva HP. BioSPPy: A Python toolbox for physiological signal processing. *SoftwareX*. 2024 May;26:101712.
77. Makowski D, Pham T, Lau ZJ, Brammer JC, Lespinasse F, Pham H, et al. NeuroKit2: A Python toolbox for neurophysiological signal processing. *Behav Res Methods*. 2021 Aug;53(4):1689–96.

78. Liu F, Xia S, Wei S, Chen L, Ren Y, Ren X, et al. Wearable Electrocardiogram Quality Assessment Using Wavelet Scattering and LSTM. *Front Physiol.* 2022 June 30;13:905447.
79. Strackiewicz M, Huang EJ, Onnela JP. A “one-size-fits-most” walking recognition method for smartphones, smartwatches, and wearable accelerometers. *Npj Digit Med.* 2023 Feb 23;6(1):29.
80. Desai AD, Yaw TS, Yamazaki T, Kaykha A, Chun S, Froelicher VF. Prognostic Significance of Quantitative QRS Duration. *Am J Med.* 2006 July;119(7):600–6.
81. Kurl S, Mäkitallio TH, Rautaharju P, Kiviniemi V, Laukkanen JA. Duration of QRS Complex in Resting Electrocardiogram Is a Predictor of Sudden Cardiac Death in Men. *Circulation.* 2012 May 29;125(21):2588–94.
82. Magnani JW, Wang N, Nelson KP, Connelly S, Deo R, Rodondi N, et al. Electrocardiographic PR Interval and Adverse Outcomes in Older Adults: The Health, Aging, and Body Composition Study. *Circ Arrhythm Electrophysiol.* 2013 Feb;6(1):84–90.
83. Schumacher K, Dagues N, Hindricks G, Husser D, Bollmann A, Kornej J. Characteristics of PR interval as predictor for atrial fibrillation: association with biomarkers and outcomes. *Clin Res Cardiol.* 2017 Oct;106(10):767–75.
84. Emrich J, Gargano A, Koka T, Muma M. Physiology-Informed ECG Delineation Based on Peak Prominence. In: 2024 32nd European Signal Processing Conference (EUSIPCO) [Internet]. Lyon, France: IEEE; 2024 [cited 2025 Sept 16]. p. 1402–6. Available from: <https://ieeexplore.ieee.org/document/10715353/>
85. Harmon D, L Dugan J, Carter R, Kashou A, Friedman P, Zachi Attia A. Performance And Accuracy Of A Smart Watch Single-lead ECG: A Pilot Study [Internet]. 2022 [cited 2025 Sept 19]. Available from: <https://www.morressier.com/article/6261147764d859b4c3959586>
86. Velraeds A, Strik M, Van Der Zande J, Fontagne L, Haissaguerre M, Ploux S, et al. Improving Automatic Smartwatch Electrocardiogram Diagnosis of Atrial Fibrillation by Identifying Regularity within Irregularity. *Sensors.* 2023 Nov 20;23(22):9283.
87. Jarchi D, Casson AJ. Towards Photoplethysmography-Based Estimation of Instantaneous Heart Rate During Physical Activity. *IEEE Trans Biomed Eng.* 2017 Sept;64(9):2042–53.
88. Malik M, Bigger JT, Camm AJ, Kleiger RE, Malliani A, Moss AJ, et al. Heart rate variability: Standards of measurement, physiological interpretation, and clinical use. *Eur Heart J.* 1996 Mar 1;17(3):354–81.
89. Zheng X, Dwyer VM, Barrett LA, Derakhshani M, Hu S. Adaptive notch-filtration to effectively recover photoplethysmographic signals during physical activity. *Biomed Signal Process Control.* 2022 Feb;72:103303.
90. Zhao L, Liang C, Huang Y, Zhou G, Xiao Y, Ji N, et al. Emerging sensing and modeling technologies for wearable and cuffless blood pressure monitoring. *Npj Digit Med.* 2023 May 22;6(1):93.
91. Subramanian A, et al. Effect of change in body position on resting 12-lead ECG. *Natl J Clin Anat.* 2016;5(2):65–70.